

Light scattering and structure in a deoxyribonucleic acid solution

R. Giordano,* F. Mallamace,* N. Micali, and F. Wanderlingh

Istituto Tecniche Spettroscopiche del Consiglio Nazionale delle Ricerche, I-98100 Messina, Italy

G. Baldini and S. Doglia

Istituto di Fisica, Università degli Studi di Milano e Gruppo Nazionale Struttura della Materia, Consiglio Nazionale delle Ricerche, I-20133 Milano, Italy

(Received 10 May 1983)

Structural properties of macromolecular solutions have been investigated with a wide variety of techniques, among which light scattering is one of the most powerful. In the present paper we report the results of both elastic and quasielastic light scattering in a DNA solution at small angles. It is shown that in solution the macromolecules arrange themselves in an ordered structure that extends over semimacroscopic distances. The comparison between the static and dynamic response allows a better understanding of the physical meaning to be attributed to the structure, in terms of a \vec{k} -dependent characteristic time for the regression of fluctuations.

I. INTRODUCTION

In the last several years macromolecular solutions have been investigated from the structural point of view using many different techniques, such as viscosity measurements,¹⁻³ light scattering,^{2,4} neutron scattering,⁵ acoustic absorption,⁶ etc. The obtained results show unambiguously that the macromolecules tend to form a quite stable, solidlike lattice composed of interacting clusters.

The structure is of the kind called "thixotropic" because it is stable against sufficiently small disturbances but can be easily destroyed, e.g., by mechanically shaking the sample. As a rule the structure builds up in a time that ranges from some tens of minutes to many hours, depending on the kind of macromolecule. As the structure builds up, the physical response of the system changes accordingly.

At present the following macromolecules have been investigated: lysozyme, bovine serum albumine (see Refs. 1-6), and hemoglobin.⁷ A comparison of results seems to indicate common behavior, although the characteristic dimension implied in the structure (i.e., the size of the cluster and the intercluster spacing) change from one macromolecular solution to another. As a rule it seems that the characteristic dimension roughly scales as the dimension of the single macromolecule.

The results obtained in the experiment reported in the present work contribute positively to such a point of view. In fact it is shown that the solution of DNA exhibits the same kind of structural behavior found in other macromolecular solutions on a larger scale due to the larger dimension of the DNA molecule.

In the present paper we report results obtained both with elastic and quasielastic light scattering. In the first case the so-called static structure factor $S(\vec{k})$ can be measured, while in the second kind of experiments the dynamical properties, in the hydrodynamical realm, can be inferred. However, as we shall see, the two kinds of measurements are strictly correlated.

As far as the quasielastic scattering is concerned, we measure the autocorrelation function $f(\tau)$ of the light in-

tensity scattered at fixed value of the exchange wave vector \vec{k} . In a system dominated by a purely diffusive Brownian motion, $f(\tau)$ behaves exponentially, the time constant being simply related to the diffusion coefficient $\Gamma = Dk^2$. However, in the large majority of physical systems the situation is more or less complicated among other things. In such a case the simple scheme sketched above is no longer valid. The autocorrelation function becomes more complicated than a simple exponential decay, and its behavior turns out to be strongly \vec{k} dependent. The concept of a diffusion coefficient becomes itself rather questionable. The introduction of an "effective" diffusion coefficient D_{eff} which depends on the structural properties of the system was proposed⁸: $D_{\text{eff}} = D_0/S(\vec{k})$. An example of a situation of this kind is known as "de Gennes narrowing" according to which the width of the quasielastic central line is narrowed at the \vec{k} values at which the structure factor $S(\vec{k})$ shows a maximum.

From the results obtained we will show, among other things, that such a concept can be applied at least as a first approximation. However, the behavior of the autocorrelation functions turns out to be more complicated than that predicted in the simple theory of Ref. 8. In particular, there is evidence for modes centered at frequencies different from zero. In other words, the behavior of the systems also shows, together with diffusive modes, propagating modes sustained by the structure.

In a sense we believe that the concept is to be reversed. The dynamical properties of the system determine, in a statistical sense, the structural behavior. A structure in the system can be thought of as originating from some contributions of the (spatial) spectrum of fluctuations whose characteristic regression time is larger than that of other components and that behave like phonons.

II. SAMPLE PREPARATION AND EXPERIMENTAL PROCEDURE

Sodium salt "highly polymerized" calf thymus DNA was purchased from Sigma Chemical Co. and used

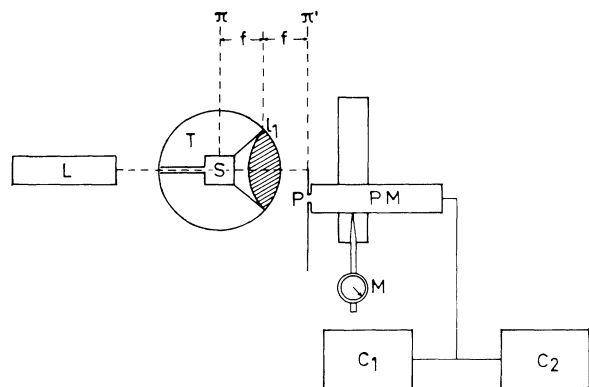


FIG. 1. Schematic view of experimental apparatus. *L*, 5 mW He-Ne laser; *T*, thermostat; *S*, Sample; *l*, Fourier-transform lens; π and π' , local planes; *P*, pinhole; *PM*, photomultiplier; *M*, micrometer; *C*₁, counter for intensity measurement; *C*₂, correlator.

without further purification. DNA was dissolved in phosphate buffers containing 7 mM Na₂HPO₄, 2 mM NaH₂PO₄, and 1 mM Na₂EDTA (pH=7.2, ionic strength ≈ 0.026), and filtered through a 1.2- μ m pore-size Millipore filter in order to eliminate foreign particles. DNA concentrations of 150 μ M (moles of phosphates) as determined by optical absorbance (molar extinction coefficient at 260 nm = 6412 M⁻¹ cm⁻¹, Ref. 9) were employed.

In order to check for the presence of denatured DNA, the hyperchromicity of the solution was checked by the method of alkali-metal denaturation reported in Ref. (10): DNA resulted free from denatured DNA.

Let us now discuss briefly the optical arrangement. Because of the relatively large size of DNA molecules as compared with, e.g., lysozyme or BSA, it is assumed that the length implied in a possible structure (cluster size, intercluster distances, etc.) is also correspondingly scaled. For example, such a scaling occurs in lysozyme and BSA solution.

Preliminary measurements confirm such a point of view. The intensity of light scattered by the DNA solution turns out to be strongly anisotropic and mainly directed forward. Then the necessity arises of making precise measurements at very low scattering angles.

For this reason we use a technique that makes use of the optical Fourier transform. The scattering volume is in the first focal plane of a converging lens so that in the second focal plane the distribution of intensity corresponds to the Fourier transform of the scattered field. Here a small pinhole (50 μ m in diameter) creates the required scattering angle. In our case a displacement of 1 mm in the second focal plane corresponds to a variation of 1° in the scattering angle so that the pinhole creates an angle with an uncertainty of 5×10^{-3} deg. The displacement of the pinhole by a micrometer can be controlled with a precision of the same order of magnitude. A schematic view of the experimental apparatus is sketched in Fig. 1.

As far as the quasielastic measurements are concerned we use a light-beating technique in the homodyne mode by

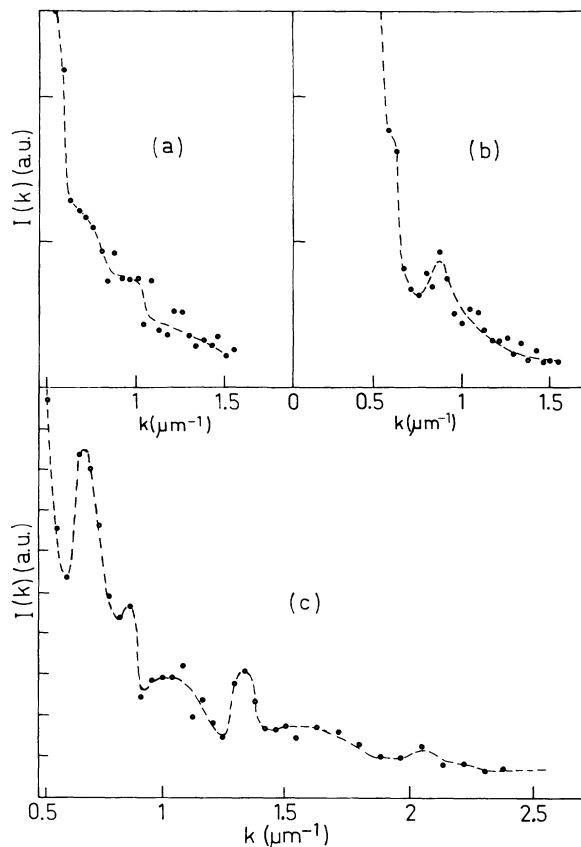


FIG. 2. Scattered intensity as a function of exchanged wave vector. (a), 15 min after the preparation of sample; (b), after 2h, 30 min; curve (c), after 30 h. Dashed lines are eye guides.

measuring the autocorrelation function of the photocurrent. We use a 5 mW He-Ne laser and a homemade clipped correlator of 120 channels together with a single-photon counting photomultiplier.

Calling n_i the number of photons detected in the i th sampling time, n_i^c the number of clipped counts in the same interval, and s the total number of sampling times, the autocorrelation function ranges from the value $\langle n_i n_i^c \rangle = (\sum n_i n_i^c) / s$ at time zero, to the value $\langle n_i \rangle \langle n_i^c \rangle = (\sum n_i) (\sum n_i^c) / s^2$ as the time goes to infinity. The correct evaluation of the latter value [i.e., the direct current (dc) term that is to be subtracted from experimental data] is of paramount importance. We control such a value both from the formula sketched above and by the use of four "delayed channels" whose position in time corresponds to 600 channels. The correspondence between the two values ensures that the correlation function actually is almost entirely displayed in the 120 channels of our correlator.

III. EXPERIMENTAL RESULTS AND DISCUSSION

A. Elastic scattering

The experimental data obtained in the elastic light scattering experiments are shown in Fig. 2. The various

curves reported here represent the time evolution of the system. Actually we perform measurements of the scattered intensity as a function of the scattering angle, at different delay times, starting from the preparation of the sample.

The general features, as expected from considerations sketched in Sec. I, can be easily shown. There is a strong indication of the existence of a more-or-less ordered structure, and the evidence for a structural effect becomes clearer and clearer as the delay time increases. Mechanically shaking the sample, the initial conditions are restored.

Measurements of the kind reported in Fig. 2 have been repeated several times, in order to be sure of the reproducibility of the results. Also control measurements are made using pure water in order to exclude hypothetical spurious effects due to misalignment, diffraction, etc.

In the sequel we discuss in detail the experimental results obtained after a very long delay time, i.e., in a stationary situation in which the structure in the system is fully developed [Fig. 2(c)]. The experimental data are taken at different scattering angles starting from 1° up to 15° . However, the data at very small angles (less than about 3°) cannot be used because of the stray contribution, due to the incident beam, at 0° .

The experimental curve clearly indicates the presence of a form factor together with a structure factor. The latter, in particular, is well evidenced by the presence of peaks at $K = 0.69 \times 10^4$, 1.38×10^4 , and $2.07 \times 10^4 \text{ cm}^{-1}$.

Let us sketch briefly the theoretical formalism that can be used to discuss elastic scattering. We consider, in principle, our system as a density distribution $\rho(\vec{r})$ of point scatterers (single molecules or even segments of a molecule), the scattered intensity of a volume element $d\vec{r}$ being proportional to $\rho(\vec{r})d\vec{r}$. Then the field scattered for a given value \vec{K} of the exchange wave vector will be given by

$$E(\vec{K}) = \int e^{i\vec{K} \cdot \vec{r}} \rho(\vec{r}) d\vec{r}, \quad (1)$$

the integral being made over the scattering volume.

Let us consider a frame of reference with the z axis, for instance, parallel to \vec{K} . Then the density can be integrated with respect to x and y . We put

$$\bar{\rho}(z) = \int \rho(x, y, z) dx dy, \quad (2)$$

so that

$$E(\vec{K}) = \int e^{iKz} \bar{\rho}(z) dz. \quad (3)$$

For the light intensity, one obtains

$$\mathcal{I}(\vec{K}) = \int e^{iK(z-z')} \bar{\rho}(z) \bar{\rho}(z') dz dz'. \quad (4)$$

Calling $\xi = z - z'$, one obtains

$$\mathcal{I}(\vec{K}) = \int e^{iK\xi} C(\xi) d\xi, \quad (5)$$

where

$$C(\xi) = \int \bar{\rho}(z) \bar{\rho}(z + \xi) dz \quad (6)$$

is the spatial autocorrelation function of the "planar den-

sity" $\bar{\rho}(z)$. Equation (5) shows that the scattered intensity reproduces the spatial Fourier transform of the density autocorrelation function, i.e., by the Wiener-Kintchine theorem, the power spectrum of the density distribution. It can also be shown that $\mathcal{I}(\vec{K})$ will be sizably different from zero only if the autocorrelation $C(\xi)$ is of finite range, the latter being not too different from K^{-1} .

Now the appearance of periodical peaks in the experimental values of $\mathcal{I}(\vec{K})$ indicate the occurrence of a periodic structure for the autocorrelation $C(\xi)$ and, therefore, for the $\bar{\rho}(z)$. The $C(\xi)$ would be obtainable by Fourier transforming the experimental curve $\mathcal{I}(\vec{K})$. Unfortunately such a procedure cannot be used with the required accuracy because of the discreteness of experimental data points, of the unavoidable statistical error, and mainly because of the absence of data in the region $K \rightarrow 0$ (i.e., for scattering angles less than about 3°).

Therefore, we try to construct a model for the $\bar{\rho}(z)$ on the basis of considerations sketched in Sec. I. We assume that the function $\bar{\rho}(z)$ is of the kind

$$\bar{\rho}(z) = \sum_{-\infty}^{+\infty} \text{rect}(a, z_n), \quad (7)$$

where $\text{rect}(a, z_n)$ is the rectangle function of width a centered at the points z_n . In turn

$$z_n = nL + \sum_{i=0}^n \epsilon_i, \quad (8)$$

where $\epsilon_0 = 0$, $z_0 = 0$. Such a model simulates an array of clusters of size a spaced by a fluctuating distance of mean value L , ϵ_i being a stochastic variable.

The Fourier transform of $\bar{\rho}(z)$ turns out to be

$$\begin{aligned} \bar{\rho}(K) &= a \frac{\sin(Ka/2)}{Ka/2} \sum_{-\infty}^{+\infty} e^{iKz_n} \\ &= a \frac{\sin(Ka/2)}{Ka/2} \sum_{-\infty}^{+\infty} e^{inKL} e^{iK\Delta_n}, \end{aligned} \quad (9)$$

where $\Delta_n = \sum_{i=0}^n \epsilon_i$ is again a stochastic variable.

The structure factor $S(\vec{K})$ is the power spectrum of $\bar{\rho}(z)$, i.e., the square modulus of $\bar{\rho}(K)$:

$$S(\vec{K}) = a^2 \left[\frac{\sin(Ka/2)}{Ka/2} \right]^2 \sum_{n, n' = -\infty}^{+\infty} e^{iK(n-n')L} e^{iK(\Delta_n - \Delta_{n'})}. \quad (10)$$

Notice that the $S(\vec{K})$ turns out to be the product of the sine that represents the "form factor" of the cluster, times the structure factor of the cluster ensemble. Equation (10) represents the instantaneous behavior of the system.

Actually one has to perform a mean because of the finite time of observation. Therefore we calculate

$$\langle e^{iK(\Delta_n - \Delta_{n'})} \rangle = \langle e^{iK\Delta_n} \rangle \langle e^{-iK\Delta_{n'}} \rangle, \quad (11)$$

having made the hypothesis that the stochastic variables Δ_n are completely uncorrelated. Obviously such a hypothesis is only a first approximation. We will see in Sec. IIIB that there is evidence for a dynamic correlation be-

tween neighboring clusters. However, such a correlation, if it exists, extends only over a short range. By such a hypothesis we can write

$$\langle e^{iK\Delta_n} \rangle = \int_{-\infty}^{+\infty} e^{iK\Delta_n} p(\Delta_n) d\Delta_n, \tag{12}$$

where $p(\Delta_n)$ is the probability distribution function for the stochastic variable Δ_n . We suppose that the fluctuations ϵ_i are Gaussian, with rms σ . Therefore, also, $p(\Delta_n)$

is a Gaussian distribution with rms $\sigma\sqrt{n}$, and we obtain

$$\begin{aligned} \langle e^{iK\Delta_n} \rangle &= \frac{1}{\sigma} (n)^{-1/2} \int_{-\infty}^{+\infty} e^{iK\Delta_n} e^{-\Delta_n^2/n\sigma^2} d\Delta_n \\ &= e^{-nK^2\sigma^2/4}. \end{aligned} \tag{13}$$

The same results hold for $\langle e^{-iK\Delta_n} \rangle$.

For the calculation of the power spectrum, one obtains

$$\sum_{n,n'=-\infty}^{+\infty} e^{iK(n-n')L} e^{-(n-n')K^2\sigma^2/4} = \sum_{n=-\infty}^{+\infty} e^{n(iKL - K^2\sigma^2/4)} \sum_{n'=-\infty}^{+\infty} e^{-n'(iKL + K^2\sigma^2/4)}, \tag{14}$$

where as far as the Gaussian terms are concerned, n is to be considered always positive. Because of such evenness, only the real part of each sum survives, and one can write

$$S(\vec{K}) = 4 \operatorname{Re} \sum_0^{\infty} e^{n(iKL - K^2\sigma^2/4)} \operatorname{Re} \sum_0^{\infty} e^{-n(iKL + K^2\sigma^2/4)} a^2 \left[\frac{\sin(Ka/2)}{Ka/2} \right]^2. \tag{15}$$

The sums are geometrical series that are absolutely convergent, with the same real part

$$\operatorname{Re} \sum_0^{\infty} e^{n(iKL - K^2\sigma^2/4)} = \operatorname{Re} \frac{1}{1 - e^{iKL - K^2\sigma^2/4}} = \frac{1}{1 - 2e^{-K^2\sigma^2/4} \cos(KL) + e^{-K^2\sigma^2/2} \sin^2(KL)},$$

so that one finally obtains (apart from a normalization factor)

$$S(\vec{K}) = \left[\frac{\frac{\sin(Ka/2)}{Ka/2} [1 - e^{-K^2\sigma^2/4} \cos(KL)]}{1 - 2e^{-K^2\sigma^2/4} \cos(KL) + e^{-K^2\sigma^2/2}} \right]^2. \tag{16}$$

Notice that (i) for large values of σ , only the form factor survives. One is concerned by the scattering of a single cluster, randomly distributed, (ii) for $KL = 2n\pi$, the $S(\vec{K})$ shows peaks whose height, modulated by the form factor, tends to infinity (δ functions) if $\sigma \rightarrow 0$. One is concerned with the scattering of an infinite, perfect diffraction grating. In Fig. 3 we show the comparison between experimental data and Eq. (16). The numerical data implied in the fit are $a = 2 \mu\text{m}$, $L = 9.5 \mu\text{m}$, and $\sigma = 3 \mu\text{m}$.

It can be seen that there is qualitative agreement, although the details of experimental data are scarcely reproduced by the theoretical curve. In particular, the second

peak and the structures between the peaks are not shown by Eq. (16). Obviously the strong rise in experimental data that takes place at very small scattering angles is due to the unavoidable contribution of the main beam, as mentioned above, and cannot be taken into account. Apart from the uncertainty in the experimental data, it is possible that the model contained in Eq. (16), although qualitatively correct, is too rough. In particular, we recall that we neglect any correlation between displacement of neighboring clusters. In order to test the relevance of correlations, it is possible to modify the model by looking at the extreme opposite situation in which a perfect correlation exists up to a given range. We obtain such a model by setting $\epsilon_i = 0$ for $i \leq s$. In such a case in Eq. (14) only the first s terms practically survive in the sum (with $\sigma = 0$). The remaining part of the system is seen as a completely disordered ensemble of clusters that gives contributions only to the form factor.

From the physical point of view the latter model identifies the system as an ensemble of diffraction gratings of finite length equal to sL , the different gratings being completely uncorrelated clusters. In such a case the structure factor becomes (apart from a normalization factor)

$$S(K) = \left[\frac{\sin(Ka/2)}{Ka/2} \right]^2 \left[\left(\sum_{n=0}^s \cos(nKL) \right)^2 + A \right], \tag{17}$$

where A represents the contribution to the structure factor of the uncorrelated clusters.

In Fig. 4 we report two fits of experimental data to Eq. (17) with the values of $s = 2$ and 3 (i.e., strong correlation in arrays of 3 and 4 clusters, respectively). It can be seen that a quite good agreement exists. In particular, the fits also reproduce the details of experimental data consisting in secondary peaks between the main peaks that occur as $KL = 2n$.

In the used solution, the DNA molecules have a molec-

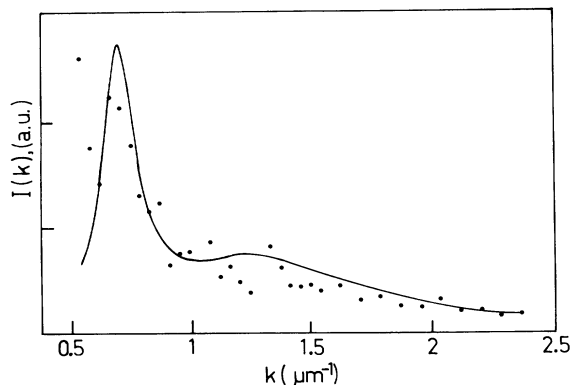


FIG. 3. Fitting of experimental data with a model structure without correlation (see text).

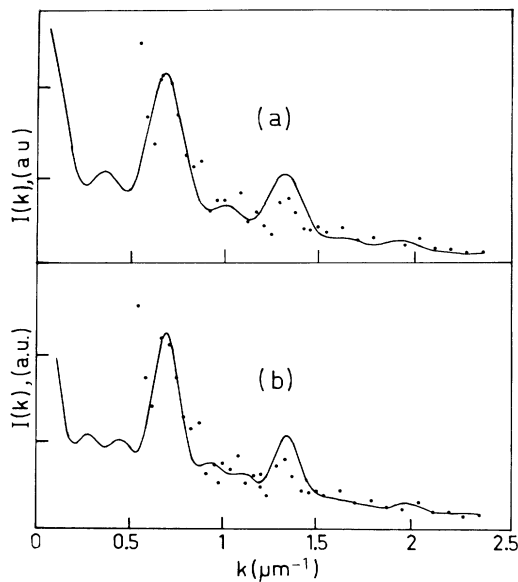


FIG. 4. Fitting of experimental data with a correlated model structure (see text). (a) and (b) refer to two different ranges of correlation.

ular weight of about 10^7 and a radius that can be estimated to be $0.26 \mu\text{m}$. At a concentration of about $100 \mu\text{M}$ (in phosphate), one can calculate a mean distance of $0.7 \mu\text{m}$. On the contrary, our experimental results indicate the existence of "scatterers" of about $2 \mu\text{m}$ spaced $9 \mu\text{m}$ apart. The fits with Eq. (17) clearly indicate the existence of such an ordering over sizable distances, in comparison with the more disordered situation implied in the fit with Eq. (16).

B. Dynamical behavior

The dynamical behavior of our system is investigated with the experimental observation of the spectrum of the inelastically scattered light (Rayleigh line) performed with the optical-beating technique through a correlator, as described in Sec. II.

Let us recall briefly the kind of information given by such a technique. There are two basic processes (obviously having a common origin) that give rise to a frequency shift in the scattered light: harmonic motion of scatterers that superimpose their own frequency on the scattered light, and displacement of scatterers that gives rise to a Doppler shift. In the first case the shift is independent from the amplitude of oscillations, while in the second it is proportional to the velocity. Actually the two processes change continuously from one to the other, the transition depending on the amplitude of oscillation.¹¹

Now, in the case in which the scatterers obey a (generalized) Langevin equation, i.e., in the case of a purely diffusive Brownian motion, it can be demonstrated that the autocorrelation function of scattered intensity obeys an exponential law

$$F(\tau) = \int_0^\infty \mathcal{I}(t)\mathcal{I}(t+\tau)dt = F_0 e^{-\Gamma\tau}. \quad (18)$$

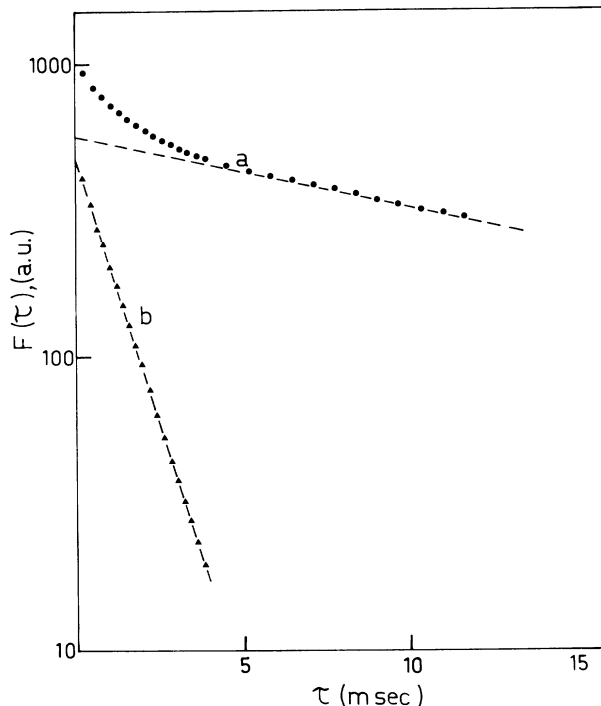


FIG. 5. Autocorrelation function at $\vartheta = 90^\circ$. (a), Experimental data (dc term subtracted). (b) Difference between experimental data and long-time exponential behavior.

In Eq. (18) the dc contribution has been subtracted, and the time constant Γ is simply related to the diffusion coefficient D :

$$\Gamma = DK^2, \quad (19)$$

K being, as before, the exchange wave vector.

However, such a simple result is jeopardized if the system shows structural properties, interactions, etc. In particular, the dependence of $F(\tau)$ from the exchange wave vector K is no longer given by Eq. (19), and the meaning of the diffusion coefficient itself becomes quite unclear.

In recent years some measurements of the diffusion coefficient of DNA have been performed by using a correlation spectroscopy technique.^{12,13} The data, however, are taken for exchange wave vectors larger than those of interest in the present work. As a consequence, the presence of an ordered structure, as revealed in the present work, is absent. In addition, the authors force the experimental correlation function to be fit to a simple exponential decay plus a constant

$$F(\tau) = Ce^{-\Gamma\tau} + B,$$

where both Γ and B are considered as fit parameters.

For comparison we report in Fig. 5 a test measurement performed at an angle of 90° (exchange wave vector $\approx 3.36 \times 10^{10} \text{ cm}^{-2}$) in which the subtracted dc term has been obtained, as sketched in Sec. II both from the indication of the delayed channels and from the calculation of $\langle n_i \rangle \langle n_i^c \rangle$. A nonexponential behavior is quite evident.

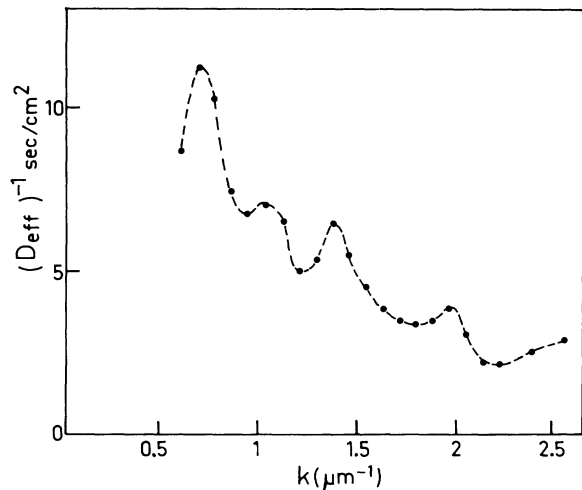


FIG. 6. Inverse of the "effective" diffusion coefficient vs exchanged wave vector.

The function can be fitted quite well with at least two exponentials:

$$F_{90^\circ}(\tau) = 0.47e^{-55.6\tau} + 0.53e^{-833.2\tau}.$$

A "diffusion coefficient," calculated from the faster decaying term, furnishes the value $D = 1.24 \times 10^{-8} \text{ cm}^2/\text{sec}$ that is of the correct order of magnitude if compared with data reported in the literature.

It has been shown^{8,14} that an "effective" diffusion coefficient D_{eff} can be defined for a model in which the motion of the scatterers can be decomposed into a "slow" and a "fast" component. The latter mainly refers to a random motion around an equilibrium position determined by nearest-neighbors interaction, while the former takes into account the displacement of the equilibrium position. The effective diffusion coefficient turns out to be inversely proportional to the static structure factor

$$D_{\text{eff}} = \frac{D_0}{S(K)}, \quad (20)$$

D_0 being a constant. In turn, D_{eff} can be obtained from experimental data evaluating the derivative at the origin of the (normalized) autocorrelation function

$$\frac{1}{F(0)} \left[\frac{dF(\tau)}{d\tau} \right]_{\tau=0} = D_{\text{eff}} K^2. \quad (21)$$

In Fig. 6 we report a plot of $(D_{\text{eff}})^{-1}$ as a function of the exchange wave vector. A comparison with Fig. 2(c) shows very good agreement. The characteristic behavior of the structure factor is reproduced in almost all details. Such an agreement gives noticeable support to the considerations developed in Sec. III A, because the same results are obtained in two entirely different kinds of measurements.

However, there is much more information contained in the experimental data that can give useful indications about the kind of dynamics experienced by the macromolecules. In Fig. 7 we report typical autocorrelation function. It can be shown that neither a single exponen-

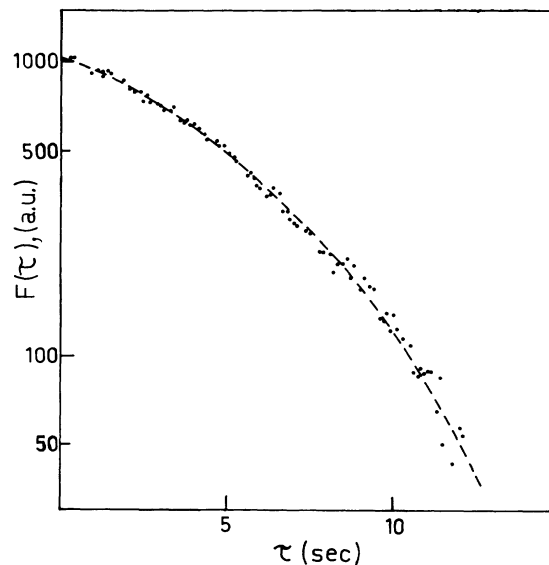


FIG. 7. Autocorrelation function at $K = 0.86 \times 10^4 \text{ cm}^{-1}$. The dc term has been subtracted. Dashed line represents the behavior of damped harmonic oscillators.

tial nor a sum of two exponentials can fit the curve. Obviously a sum of a large enough number of exponentials could fit the curve, although such a procedure does not have a clear physical meaning. Because of the existence of a thixotropic structure, the hypothesis that harmonic motion can occur seems quite reasonable. We suppose, therefore, that the scatterers can move as damped harmonic oscillators. In such a case the autocorrelation function can be calculated and turns out to be

$$F(\tau) = Ce^{-\Gamma\tau} \left[\cos(\Omega\tau) - \frac{\Omega\Gamma}{2\Gamma^2 + \Omega^2} \sin(\Omega\tau) \right], \quad (22)$$

where Γ is the damping constant and Ω the angular frequency of the oscillator.

The dashed line in Fig. 7 represents a fit of experimental data with Eq. (22). The results show that an equation, like Eq. (22), can actually represent with very good accuracy the experimental results.

It is to be noted that, according to the considerations in Sec. III A, the entire structure contributes to the intensity scattered at a given angle because of its spatial correlation. The circumstance that in such a condition an oscillating behavior can be clearly shown, implies that there are also temporal correlations in the motion of the macromolecules. In other words, the dynamics of the thixotropic structure show a collective behavior that can be described in terms of phonons.

The fitting performed in Fig. 7 can be repeated for different exchange wave vector so that a "dispersion law" $\Omega = \Omega(K)$ can be obtained. It is, however, to be noted that if in Eq. (22) the value of Γ turns out to be larger than say twice the value of Ω , the fit becomes quite insensitive to the value of Ω . For such a reason we can perform the fits only up to $K = 1.56 \times 10^4 \text{ cm}^{-1}$. The results are shown in

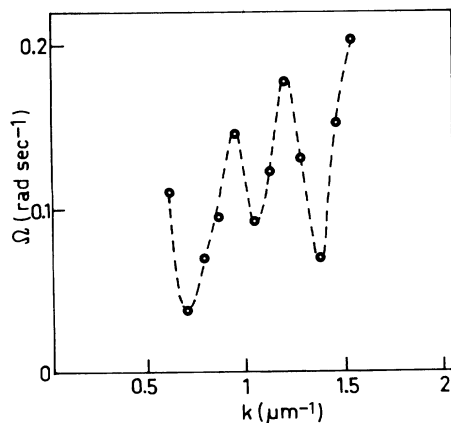


FIG. 8. Dispersion curve for collective mode in DNA solution.

Fig. 8.

A dispersion law of the kind reported in Fig. 8 has been predicted theoretically^{15,16} and shown in some experimental results on neutron scattering.¹⁷ It is interesting to note that such kinds of results arise in pure liquids only for large enough wave vectors (in the range of some \AA^{-1}), while in our case the implied values of wave vectors are much smaller. Correspondingly, the values of energy are also suitably scaled. Such a circumstance is a trivial consequence of both the largest scale of the spatial structure and the weakness of the interactions responsible for the building of the thixotropic structure.

From a theoretical point of view the first minimum in the dispersion law would correspond to the reaching of the boundary of the first Brillouin zone (i.e., the first peak in the structure factor). The presence, in our case, of successive minima is, again, to be related to the successive peaks in the structure factor, i.e., the long-range order showed in our systems.

IV. CONCLUDING REMARKS

The solution of DNA shows peculiar structural properties consisting of an ordered arrangement of macromolecules in a solidlike thixotropic structure. Such behavior seems to be a quite general property of macromolecular solutions being found in aqueous solutions of lysozyme, BSA, and hemoglobin.

In the case of DNA, due to the large scattering efficiency of the macromolecule, the elastic scattering of light gives results that allow a more careful analysis. In particular, the characteristic distance implied in the structure ($\sim 9 \mu\text{m}$) allows the detection of at least three peaks in the structure factor, so that the experimental results can be reasonably compared with a precise model. In addition, the dynamical results obtained in the quasielastic light

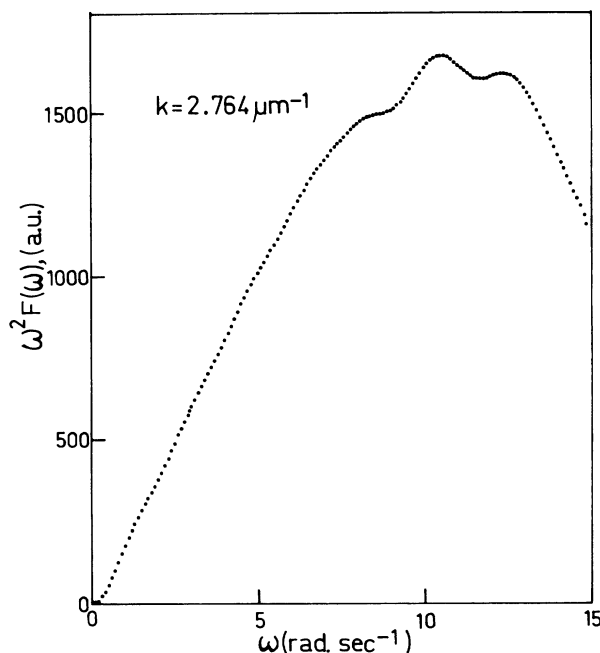


FIG. 9. Longitudinal-current autocorrelation function. The presence of peaks corresponds to different modes of the system for $K = 2.764 \mu\text{m}^{-1}$.

scattering experiments give satisfactory agreement with the model, allowing an independent evaluation of the structure factor.

It is also shown that the dynamical behavior of the system could be described in terms of collective modes (phonons), supported by the thixotropic structure. Such modes are quite evident at low values of exchange wave vector, although the increasing value of the damping constant prevent a clear evaluation of the frequency at larger values of the exchanged wave vector.

We would also note that there are strong indications of the existence of modes at higher frequency. Actually one can perform a Fourier transform of the autocorrelation function. Then a plot of such a Fourier-transform time ω^2 would correspond to the power spectrum of the correlation of longitudinal currents in the system.¹⁶ Each peak in such a curve can be related to a mode of the system. In Fig. 9 we report an example of such a procedure. However, a careful analysis of this kind requires an extremely high precision in the experimental data because the numerical Fourier transform is strongly sensitive to even very small disturbances in the data. For this reason we do not perform such an analysis here. A refined experimental procedure is at present in progress in order to obtain data of good enough quality. We would only emphasize that higher-frequency modes could be related to the intramolecular dynamics of the DNA chain, and, therefore, their investigation could be of great interest.

- *Also at Istituto di Fisica, Università degli Studi di Messina Gruppo Nazionale Struttura della Materia, I-98100 Messina, Italy.
- ¹R. Giordano, M. P. Fontana, and F. Wanderlingh, *J. Chem. Phys.* **74**, 2011 (1981).
- ²R. Giordano, G. Maisano, F. Mallamace, N. Micali, and F. Wanderlingh, *J. Chem. Phys.* **75**, 4770 (1981).
- ³R. Giordano, F. Wanderlingh, L. Cordone, and A. Cupane, *Nuovo Cimento D* **2**, 47 (1983).
- ⁴R. Giordano, F. Mallamace, A. Salleo, S. Salleo, and F. Wanderlingh, *Opt. Acta* **27**, 1465 (1980).
- ⁵R. Giordano, G. Maisano, and F. Wanderlingh (unpublished).
- ⁶R. Giordano, F. Mallamace, and F. Wanderlingh, *Nuovo Cimento D* (in press).
- ⁷R. Giordano, F. Wanderlingh, L. Cordone, and A. Cupane (unpublished).
- ⁸J. C. Brown, P. N. Pusey, J. W. Goodwin, and R. M. Otterwill, *J. Phys. A* **8**, 664 (1975).
- ⁹G. Felsenfeld, and S. Z. Hirschmann, *J. Mol. Biol.* **13**, 407 (1965).
- ¹⁰W. Muller and D. M. Grothers, *Eur. J. Biochem.* **54**, 267 (1975).
- ¹¹F. Mallamace, N. Micali, and F. Wanderlingh, *J. Opt. Soc. Am.* (in press).
- ¹²N. Parthasarathy and K. S. Schmitz, *Biopolymers* **19**, 1655 (1980).
- ¹³J. C. Thomas, S. A. Allison, and J. M. Schurr, *Biopolymers* **19**, 1451 (1980).
- ¹⁴P. S. Dalberg, A. Boe, K. A. Strand, and T. Sikkeland, *J. Chem. Phys.* **69**, 5473 (1978).
- ¹⁵K. N. Pathac, K. S. Singwi, G. Cubiotti, and M. P. Tosi, *Nuovo Cimento B* **13**, 185 (1973).
- ¹⁶J. P. Boon and S. Yip, *Molecular Hydrodynamics* (McGraw-Hill, New York, 1980), Chap. 6.
- ¹⁷W. J. L. Buyers, V. F. Sears, P. A. Lonngi, and D. A. Lonngi *Proceedings in Neutron Inelastic Scattering, Grenoble, 1972* (IAEA, Vienna, 1972), p. 399; J. B. Suck and W. Glaser, *ibid.*, p. 435.